Synthesis, ex vivo and in silico studies of 3-cyano-2-pyridone derivatives with vasorelaxant activity

ARTICLE *in* EUROPEAN JOURNAL OF MEDICINAL CHEMISTRY · OCTOBER 2013

Impact Factor: 3.45 · DOI: 10.1016/j.ejmech.2013.10.018 · Source: PubMed

8 AUTHORS, INCLUDING:

Fernando Hernandez
Universidad de Guanajuato
3 PUBLICATIONS **9** CITATIONS
SEE PROFILE

Cesar Millan
Universidad Autónoma del Estado de Morelos
22 PUBLICATIONS **158** CITATIONS
SEE PROFILE

Francisco Delgado
Escuela Naciona De Ciencias Biológicas
92 PUBLICATIONS **747** CITATIONS
SEE PROFILE

Samuel Estrada-Soto
Universidad Autónoma del Estado de Morelos
88 PUBLICATIONS **821** CITATIONS
SEE PROFILE

European Journal of Medicinal Chemistry 70 (2013) 669–676

Contents lists available at ScienceDirect

European Journal of Medicinal Chemistry

journal homepage: http://www.elsevier.com/locate/ejmech

Short communication

Synthesis, *ex vivo* and *in silico* studies of 3-cyano-2-pyridone derivatives with vasorelaxant activity

Fernando Hernández [a], Arturo Sánchez [a], Priscila Rendón-Vallejo [b], César Millán-Pacheco [c], Yolanda Alcaraz [d], Francisco Delgado [e], Miguel A. Vázquez [a,*], Samuel Estrada-Soto [b,*]

[a] Departamento de Química, División de Ciencias Naturales y Exactas, Universidad de Guanajuato, Gto. 36050, Mexico
[b] Facultad de Farmacia, Universidad Autónoma del Estado de Morelos, Cuernavaca, Mor. 62209, Mexico
[c] Facultad de Ciencias, Universidad Autónoma del Estado de Morelos, Cuernavaca, Mor. 62209, Mexico
[d] Departamento de Farmacia, División de Ciencias Naturales y Exactas, Universidad de Guanajuato, Gto. 36050, Mexico
[e] Departamento de Química Orgánica, Escuela Nacional de Ciencias Biológicas, IPN, Prol. Carpio y Plan de Ayala, 11340 México, D. F., Mexico

ARTICLE INFO

Article history:
Received 21 June 2013
Received in revised form
3 October 2013
Accepted 7 October 2013
Available online 14 October 2013

Keywords:
4*H*-Pyrans
2-Pyridones
Microwave irradiation
Vasorelaxant activity
Docking score
L-type calcium channel

ABSTRACT

An efficient and simple synthesis of 3-cyano-2-pyridone derivatives (**6a**–**f**) through 3,4-dihydropyridin-2-one oxidation process is described. A greener method to synthesize 3,4-dihydropyridin-2-one has also been developed by rearranging 4*H*-pyran (**4a**–**f**) derivatives in aqueous medium applying H_2SO_4 as the catalyst source and microwave irradiation. The vasorelaxant activity of 3-cyano-2-pyridone derivatives (**6a**–**f**) was proved on isolated thoracic aorta rat rings with and without endothelium (+E and −E, respectively) pre-contracted with noradrenaline (0.1 μM). All compounds exhibited significant concentration-dependent and endothelium-independent vasorelaxant effects being the nitro derivatives (**6a** and **f**) and compound **6d** the most potent with EC_{50} of 7, 4.4 and 5 μM, respectively. Finally, a previously described 3D model of the central pore of human L-type calcium channel (LCC), modified to be on agreement with NCBI sequence NP_005174.2 for subunit alpha-1F isoform 1, was used to dock most active compounds. **6a**, **d** and **f** lowest affinity energy structures were found docked in the same cavity conformed by IS6, IS5, IP and IIS6 helices. Nifedipine lowest energy structure was found in the cavity formed by IIS6, IIS5, IIP and IIIS6. Although nifedipine docked in a different cavity, the superposition of both, allowed us to observe that they were almost the same cavities, indicating that there exist subtle steric differences that lead to a different docking for nifedipine. All compounds docked with similar free energy of binding.

1. Introduction

Cardiovascular disease (CVD) has been recognized as the most common leading cause of mortality in developed countries. The underlying risk factors that trigger CVD are metabolic disorders (atherogenic dyslipidemia), obesity (induced by physical inactivity and caloric diet), diabetes and hypertension [1,2]. In this context, hypertension is one of the most prevalent causes that origin CVD by development of an impaired vascular relaxation process for appearance of endothelial dysfunction and oxidative stress [3]. Antihypertensive drugs influence arterial blood pressure at four effectors' sites: the resistance vessels, the capacitance vessels, the heart, and the kidney [4].

So, new antihypertensive agents with new or known therapeutic targets are needed to control hypertension more effectively, with less adverse effects and neutral impact on known cardiovascular risk factors. Thus, in an attempt to found novel antihypertensive compounds with vasorelaxant activity, we decided to design 3-cyano-2-pyridone hybrids derivatives as calcium channel blockers and possible PD3 and PD4 inhibitors taken in account nifedipine, milrinone and amrinone [5–8]. 2-pyridones constituted an important type of heterocyclic that have shown variety of biological activities [5]. They work as specific phosphodiesterase (PDE3) inhibitors and are good alternative to classic digitalis glycosides for the acute treatment of congestive heart failure (CHF) i.e. amrinone and milrinone (Fig. 1) [6,7]. In addition, nifedipine (Fig. 1) is a dihydropyridine L-type calcium channel (LCC) blocker. Its main uses are as an antianginal (especially in Prinzmetal's angina) and

* Corresponding authors.
E-mail addresses: mvazquez@ugto.mx (M.A. Vázquez), enoch@uaem.mx (S. Estrada-Soto).

0223-5234/$ – see front matter © 2013 Elsevier Masson SAS. All rights reserved.
http://dx.doi.org/10.1016/j.ejmech.2013.10.018

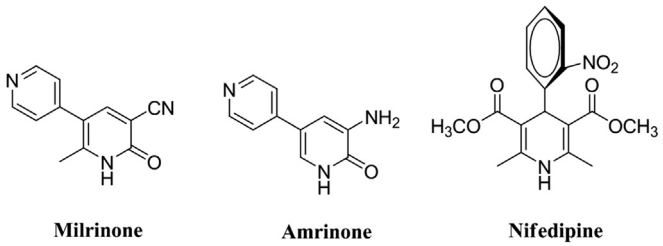

Fig. 1. Structure of milrinone, amrinone and nifedipine.

antihypertensive, although a large number of other indications have recently been found for this agent, such as Raynaud's phenomenon, premature labor, and painful spasms of the esophagus such as in cancer and tetanus patients. It is also commonly used for the small subset of pulmonary hypertension patients whose symptoms respond to calcium channel blockers [8].

The most common method used to synthetize 2-pyridones is the Michael addition of acetonitrile derivatives to an appropriate α,β-unsaturated carbonyl substrate and subsequent hydrolytic cyclization followed by oxidative aromatization [9–11]. Alternatively, β-oxo amides under Vilsmeier conditions are used to produce 2-pyridones [12]. Other notable methods starting from the Blaise reaction intermediate were reported [13]. However, many of the established methods carried out this procedure under harsh reaction conditions. On the other hand, one of the objectives in modern synthetic organic chemistry includes leading reactions with effective, clean, and environmentally safer methodologies. It is appropriate to mention that the revision of fundamental synthetic reactions using different energy source [14], represents one of the main subjects of our research group in order to contribute to the development of environmentally benign methods. Thus, various reactions have been studied: among them the Knoevenagel condensation [15–17], the Biginelli reaction [18], the formation of *N*-benzylideneanilines [19], 4*H*-pyran [20], and the Diels–Alder reaction [21].

2. Results and discussion

2.1. Chemistry

Our group previously reported the synthesis of 4*H*-pyrans derivatives and 2-pyridones using infrared irradiation [20], and we projected that a rearrangement of **4a**–**f**, and subsequent oxidation reaction, would provide a synthetic route for 3-cyano-2-pyridone (**6a**–**f**) under microwave irradiation (Scheme 1).

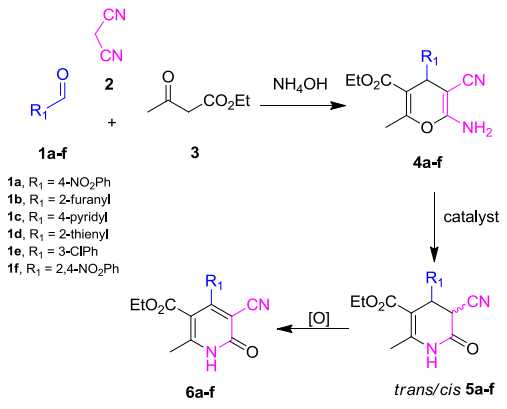

Scheme 1.

Table 1
Comparison of different sources of energy for conversion of **4a** to **5a**.[a]

Entry	Source energy	T (°C)	Reaction time	Yield (%)[b]
1	Infrared (50 V)	80	7 min	80
2	Conventional	80	30 min	72
3	Microwave	100	5 min	86
4	Room temperature	25	7 h	8

[a] All entries were carried out using *p*-toluenesulphonic acid as catalyst in ethanol as solvent.
[b] Determined by ^{1}H NMR of the recrystallization of crude reaction, corresponding to the mixture of *trans*/*cis* adducts.

It was envisaged sequential ring-opening followed by ring-closure process of 4*H*-pyran **4a**. To find a suitable catalyst for this rearrangement, we initially screened the reaction with *p*-toluenesulphonic acid as catalyst [22], using microwave irradiation as energy source at 100 °C, for 5 min, in the absence of solvent. The desired pyridone **5a** was obtained as a mixture of diastereoisomers *trans*/*cis* in low yield (60%), as judged from ^{1}H NMR (300 MHz) analysis of the crude reaction (Supplementary information).

In an attempt to obtain a homogeneous reaction by improved the adduct obtained, the reaction was performed with $CHCl_3$, THF, CH_3CN, dioxane, water and ethanol to found the right catalytic activity of acid and the best suited medium of transformation. We found that the reaction using ethanol (86% yields) as the solvent resulted in higher yields than any other solvent.

To demonstrate the efficiency and applicability of the microwave irradiation we also compared different sources of energy. The comparison of the yields and reaction times shows that by using infrared [23] and microwaves irradiation the reaction time is shortened and the product yielded is increased (Table 1, entry 1, 3).

In addition, we screened a number of Brönsted acids for efficient ring-opening/ring-closing of **4a**. Also, it was studied the catalytic activity of iodine (Lewis acid) over the reaction using microwave irradiation. Hydrochloric acid was found slightly better (yield 79%), however best results were obtained with sulfuric acid (yield 95%). The latter catalyst in 10 mol% was sufficient to push the reaction forward, nevertheless and increasing in the amounts of catalyst (30 mol%) did not improved the yield (95%). Reducing the amount of catalyst to 5 mol%, resulted in a lower yield (65%). Moreover, the inclusion of iodine in the reaction resulted in a poor conversion of **5a** (yield 57%). Thus, reactions were carried out with 10 mol% of the catalyst and microwave irradiation was used as the energy source.

The use of optimal experimental conditions described later (microwave irradiation, 5 min, 100 °C, H_2SO_4–EtOH) for the

Table 2
Relation between diastereoisomers *trans*/*cis* **5a**–**f** by NMR.

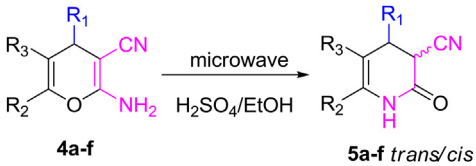

Entry	Product	Yield (%)[a]	Adducts (*trans*/*cis*)
1	**5a**	95	84/16
2	**5b**	87	82/18
3	**5c**	95	84/16
4	**5d**	88	89/11
5	**5e**	83	80/20
6	**5f**	92	82/18

[a] Determined after re-crystallization by ^{1}H NMR, corresponding to the mixture of *trans*/*cis* adducts.

reactions of different 4*H*-pyrans **4b**–**f** afforded good yields for 3,4-dihydropyridin-2-ones **5b**–**f** as a mixture *trans*/*cis* adducts. The results (Table 2, entries 1–6) indicated that aryl or heteroaryl functional groups were all suitable for the reaction.

Compounds **5a**–**f** were isolated as a mixture *trans*/*cis* adducts, like its precursors, these had the same number of signals in the proton-decoupled ^{13}C NMR spectrum. Its ^{1}H NMR spectrum for **5a** shows the appearance of two new sets of signals at ~10.80–10.40 ppm to the protons NH (*trans*/*cis*), ~5.05–4.57 ppm (*trans* J = 7.5 Hz) and 4.67–4.35 ppm (*cis* J = 5.5 Hz). Furthermore, the infrared spectrums of **5a**–**f** displayed carbonyl absorptions at ~1721 and 1662 cm^{-1}, in contrast to the carbonyl absorption at ~1676 cm^{-1} for **4a**–**f**.

The ring-opening/ring-closing of **4a** proved to be an efficient process for building the 3,4-dihydropyridin-2-ones scaffold. That pyridine-2-ones **5a**–**f** possesses a core, which may be expected to undergo an oxidation reaction.

In order to support the aromatization the adduct **5a** was reacted with 2,3-dichloro-5,6-dicyano-1,4-benzoquinone (DDQ), in ethanol as the solvent, the test was performed with microwave energy as an alternative source (100 °C/14 psi, ethanol, 5 min), the conversion is efficient (91% yield).

In order to investigate the scope and limitations of this oxidation reaction, as well as to identify the possible effect induced by other substrates on the formation of compounds **6b**–**f**, we carried out the reaction with substrates **5b**–**f** under the same reaction conditions. A similar behavior was observed with respect to **5a**, leading to adducts **6b**–**f** as single products in comparable yields (Table 3). It is evident that the reaction proceeded smoothly for both electro rich and electro deficient aryl and heteroaryl aldehydes with reasonably good yield. The spectral data and physical properties of **6a**–**f** are showed in the Supplementary information.

2.2. Vasorelaxant effect of compounds *6a–f*

On the other hand, compounds **6a**–**f** showed a significant vasorelaxant activity in a concentration-dependent manner on the contraction induced by noradrenaline (0.1 μM, NA) (Table 4) on aorta rat rings. Compounds **6a**, **d** and **f** were the most potent, and revealed an endothelium-independent effect (Fig. 2a–c). All compounds tested were less potent than positive control **nifedipine** and carbachol, respectively. An endothelium-independent relaxation is related with a smooth muscle cells activity, which interferes on contraction processes such as α-adrenoceptors antagonism, calcium channel blockade, potassium channel opening, cAMP or cGMP increment, or Ca^{2+}-CaM complex activity inhibition [24,25]. As we described previously, 3-cyano-2-pyridone hybrids derivatives were designed as calcium channel blockers and possible PD3 and PD4 inhibitors, taken in account nifedipine (L-type calcium channel blocker), milrinone and amrinone (PD3 and PD4 inhibitors) with potential vasorelaxant and antihypertensive effects. So, we expect that some of these compounds showed vasorelaxant effect by an interference with LCC as described for nifedipine and other LCC blockers structurally related.

Table 3
Synthesis of 5-cyano-pyridin-2-ones **6a**–**f**.[a]

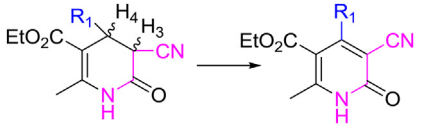

5a-f *trans*/*cis* **6a-f**

Comp.	R_1	Yield (%)[b]	m.p [°C]
6a	4-$NO_2C_6H_4$	91.0	208–210
6b	C_4H_3O	90.0	223–225
6c	C_5H_4N	84.0	174–176
6d	C_4H_3S	94.0	212–214
6e	3-ClC_6H_4	95.0	230–232
6f	2,4-$(NO_2)_2C_6H_3$	85.0	268–269

[a] The compounds (**5a**–**f**) (1 mmol), DDQ (1 mmol) were irradiated with microwaves in 3 mL ethanol at 100 °C for 5 min.
[b] Isolated yield of the pure product.

Table 4
Relaxatory effects induced by **6a**–**f** on the contraction induced by NA (0.1 μM).

	With endothelium (E+)		Without endothelium (E−)	
Contractile agent: NA 0.1 μM				
Compound	EC_{50} (μM)	Efficacy (%)	EC_{50} (μM)	Efficacy (%)
6a	7	98 ± 1.96	8.2	95 ± 0.69
6b	22	100 ± 4.18	31	93 ± 1.77
6c	270	85.47 ± 1.86	178	86.40 ± 1.84
6d	5	100 ± 2.1	12	99 ± 0.69
6e	85	97 ± 2.06	62	99 ± 2.1
6f	4.4	97 ± 3.1	3.6	99 ± 2.1
Carbachol	0.30	74.06 ± 5.7	ND	ND
Nifedipine	ND	ND	0.03	97.0 ± 2.48

2.3. Molecular docking of compounds *6a*, *d*, *f* and *nifedipine* on human L-type calcium channel

In order to explain the possible blockade of LCC of compounds **6a**, **d** and **f** as **nifedipine** does, they were docked on human calcium L-type channel to test their binding affinities. Docking studies were done over all inner cavities facing to cytoplasm without any bias to a specific cavity. Fig. 3 shows the aminoacids sequence of the helices where compounds docked by Vina. Recently, Pandey et al. [26] showed a theoretical model for N-type calcium channel. They found that their model was in agreement with previous studies on LCC [27,28]. In current work, we have used aminoacids numeration as proposed by Pandey et al. [26] for N-type, to facilitate any comparison between their results than obtained by us.

Compounds **6a**, **d** and **f** lowest affinity energy structures were found docked in the same cavity conformed by IS6, IS5, IP and IIS6 helices (Fig. 4). Whereas, **nifedipine** lowest energy structure was found in the cavity formed by IIS6, IIS5, IIP and IIIS6. Although **nifedipine** docked in a different cavity, cavities superposition allowed us to observed that they where almost the same indicating that there exists subtle steric differences that lead to a different docking for **nifedipine** (Fig. 4c). Pandey et al. [26] found that $Met^{IP.49}$, $Glu^{IP.50}$, $Thr^{IP.48}$ and $Glu^{IIP.50}$ interact with **nifedipine** by hydrogen bonds. While, we found that **nifedipine** interact with those conserved aminoacids on L-type channel ($T^{IIP,48}$, $G^{IIP,49}$ and $E^{IIP,50}$). Van der Waals interactions, that Pandey et al. [26] found, included $Ser^{IS6.15}$, $Leu^{IIS6.18}$, $Thr^{IIP.48}$, $Gly^{IIP.49}$, $Phe^{IIIS6.11}$, $Phe^{IIIS6.14}$, $Pro^{IIIS6.15}$, $Phe^{IIIS6.18}$, $Phe^{IIIS6.22}$ and $Val^{IIIS6.19}$. In present study, we did not found the same residues (due in part to the length of the helices used on the model employed), however, residues that we found were located on positions near to those proposed before [27]. For example, IIIS6 residues were located on positions from V9 to P15; while, we found residues in contact with nifedipine by Van der Waals interactions in the same range of aminoacids (I11 and I14). I11 and I14 were known positions on 1,4-dihydropyridines (as nifedipine) bind [28]. Based on previous results [26–28], we proposed that Autodock Vina reproduced completely the reported interaction between nifedipine and L-type calcium channel.

Compounds **6a**, **d** and **f** are closely structurally related and these were found on the lowest binding affinity energy obtained by

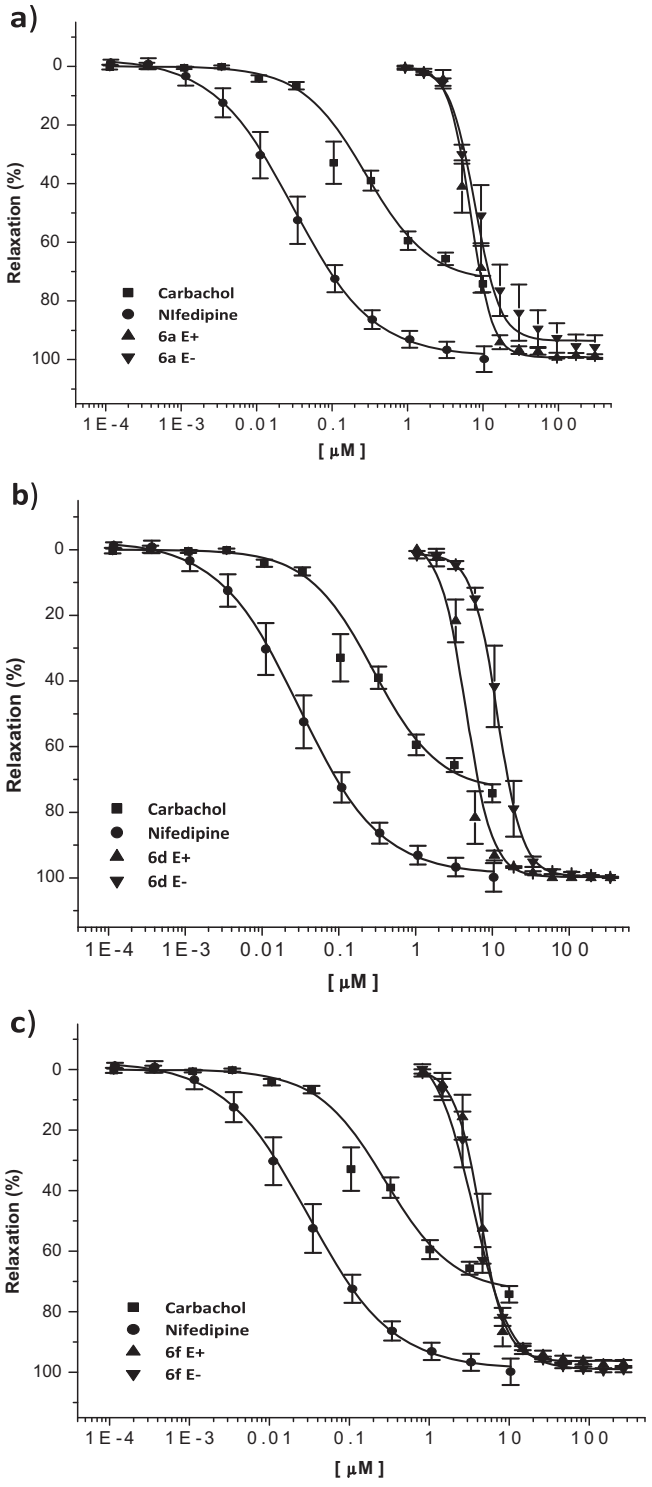

Fig. 2. Concentration–response curves of most active compounds **6a**, **d** and **f** on aorta rat rings pre-contracted with NA (0.1 μM).

Autodock Vina (−6.3, −6.6, −5.8 and −6.5 kcal/mol for nifedipine, **6a**, **d** and **f**, respectively). Using Goldmann and Stoltefuss [29] nomenclature (portside, bowspirit, starboard and stern), **6a**, **d** and **f** have a cyano and carbonyl group in the starboat side and they differ in the bowspirit group. **6a** has a NO_2 group in *para* position, while **6f** shows two NO_2 substituents in *ortho* and *para*, respectively. Moreover, **6d** change from a bencyl group to a 2-thienyl cycle. As noted in the 2D interaction diagrams and 3D molecular representations (Fig. 5), **6a** and **f** cyano group faces into the protein; meanwhile portsides faced to the aqueous side of the calcium channel (interacting by hydrogen bond with $N^{IIS6.15}$ side chain). **6a**, **d** and **f** bowspirit group faced to the cavity side (this group had interactions with $I^{IIIS6.11}$, $I^{IIIS6.14}$ {residues that have effects on dihydropyridines binding} [28] and $G^{IIS6.14}$) avoiding possible steric clashes of the NO_2 in *ortho* position from nifedipine.

On the other hand, compound **6f** shows two NO_2 groups at the bowspirit side that may provide a strong negative side, which could be neutralized by the presence of positive ions. These two NO_2 groups and their negative charge might be the reason why Autodock Vina found the cavity formed by IS6, IS5, IP and IIS6 a better location for **6f**. In this cavity, there exist an additional $N^{IIS6.15}$ that could form hydrogen bonds with a NO_2 groups. Compound **6f** were docked with the bowspirit side facing into the protein side of the channel, but the cyano group was located on a position that is not able to make the same hydrogen bond with $N^{IIS6.15}$ side. Compound **6d** docked their stern group into the protein cavity as nifedipine does, but the lack of an esther group (instead of the cyano on **6d**) reduced the number of hydrophobic interactions with protein residues that might influenced its binding affinity for protein.

In conclusion, it was designed and synthesized some hybrid milrinone–nifedipine analogs by greener method with significant potent and efficient vasorelaxant effect that could be used as Hit for the development of new analogs with more potency and efficacy than described here. Also, computational studies allowed us to hypothesize that more active compounds are acting as LCC blockers, which suggest that our compounds could be used in the treatment of hypertension and related diseases.

3. Experimental

3.1. Chemistry

Melting points were determined on an Electrothermal digital 90100 melting point apparatus and were uncorrected. The progress of the reaction and the purity of compounds were monitored by TLC with E. Merck silica gel 60-F_{254} coated aluminum sheets, in *n*-hexane/ethyl acetate (7:3), and visualized by a 254 nm UV lamp. IR spectra were recorded on a Perkin–Elmer Spectrum 100 FT-IR spectrophotometer. NMR spectra were recorded, for solutions in DMSO-d_6 and $CDCl_3$ with Me_4Si as internal standard, on Varian Gemini (300 MHz) and Varian VNMR System (500 MHz) instruments. High-resolution mass spectra (HRMS) were obtained with a JSM-GCMate II mass spectrometer, and electron impact techniques (70 eV) were employed. The 4*H*-pyrans were reported previously [20], and were used to obtained the products **6a**–**f**. CEM discover-SP microwave reactor was used for these reactions.

3.1.1. *General procedure for the preparation of ethyl-5-cyano-2-methyl-6-oxo-4-hetero and carboaryl-1,4,5,6-tetrahydropyridine-3-carboxylate (**5a**–**f**)*

3.1.1.1. Method A. A mixture of 4*H*-pyran **4a**–**f** (1.50 mmol) and concentrated sulfuric acid (10 mol%) in EtOH (3 mL) was irradiated with infrared until at 80 °C (50 V) for 15 min. The progress of the reaction was monitored by TLC (hexane/EtOAc, 7:3). The reaction was continued to carry out a recrystallization using a proportion H_2O/EtOH (95/5) to obtain the mixture of the two diastereoisomers. The obtained solid was collected by vacuum filtration; the product was allowed to dry and then quantified.

3.1.1.2. Method B. In a pressure tube for microwave reactions was placed 4*H*-pyran **4a**–**f** (1.50 mmol) and 3 mL of EtOH added. To the reaction mixture was added concentrated sulfuric acid (10 mol%).

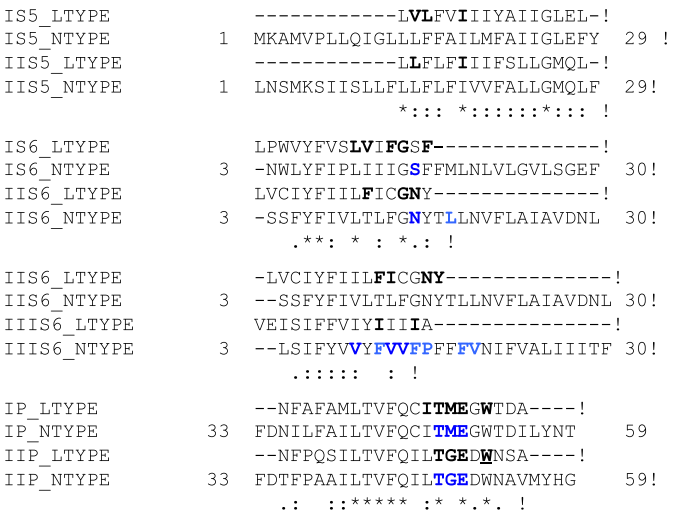

Fig. 3. Aminoacid sequence for L-type calcium channel where **nifedipine**, **6a**, **d** and **f** where found docked. Aminoacid sequence for N-type calcium channel for its corresponding helices is shown. Aminoacid sequence and numeration where taken from Pandey et al. [26]. Blue color on N-type sequences shows those residues that Pandey et al. [26] found that interact with nifedipine, and which, we also found that interact with it on L-type calcium channel. (For interpretation of the references to color in this figure legend, the reader is referred to the web version of this article.)

The reaction mixture was irradiated with microwave irradiation until a reaction temperature of 100 °C for 5 min, 39 psi, 10 W. The end of the reaction was confirmed by TLC using a 7:3 (Hex/AcOEt). The reaction was continued to carry out a recrystallization using a proportion H_2O/EtOH (95/5) to obtain the mixture of the two diastereoisomers. The obtained solid was collected by vacuum filtration; the product was allowed to dry and then quantified.

*3.1.2. General procedure for the preparation of ethyl-5-cyano-2-methyl-6-oxo-4-hetero and carbo aryl-1,6-dihydropyridine-3-carboxylate (**6a**–**f**)*

3.1.2.1. Method A. A mixture of 1,4,5,6-tetrahydropyridine (**5a**–**f**). (1.52 mmol), ethanol (3 mL) and DDQ (1.52 mmol) was irradiated with infrared until at 80 °C (50 V) for 10 min. The progress of the reaction was monitored by TLC (EtOAc/hexane 5:5). The reaction was purificated by chromatography column (hexane/AcOEt, 1/1). The obtained solid was collected after vacuum.

3.1.2.2. Method B. A mixture of 1,4,5,6-tetrahydropyridine (**5a**–**f**). (1.52 mmol), ethanol (3 mL) and DDQ (1.52 mmol) was irradiated with microwaves until at 100 °C, 39 psi, 10 W for 5 min. The progress of the reaction was monitored by TLC (EtOAc/hexane 5:5). The reaction was purificated by chromatography column (hexane/AcOEt, 1:1). The obtained solid was collected after vacuum.

*3.1.3. Ethyl-5-cyano-2-methyl-4-(4-nitrophenyl)-6-oxo-1,6-dihydropyridine-3-carboxylate (**6a**)*

Yield: 91%; brown solid; mp 208–210 °C; IR (KBr): 2254, 1651, 1283 cm^{-1}; ^1H NMR (DMSO-d_6, 200 MHz) δ 13.13 (s, 1H), 8.46 (d, J = 8.4 Hz, 2H), 7.74 (d, 2H, J = 8.4 Hz), 3.92 (q, 2H, J = 7 Hz), 2.54 (s, 3H), 0.80 (t, 3H, J = 7 Hz); ^{13}C NMR ($CDCl_3$, 50 MHz): δ 164.2, 159.4, 157.8, 154.9, 147.9, 142.8, 128.9, 123.6, 115.0, 110.9, 101.0, 61.05, 18.7, 13.1; HRMS (EI^+) calculated for $C_{16}H_{13}N_3O_5$: 327.0855, found 327.0855.

*3.1.4. Ethyl-5-cyano-4-(furan-2-yl)-2-methyl-6-oxo-1,6-dihydropyridine-3-carboxylate (**6b**)*

Yield: 90%; yellow solid; mp 223–225 °C; IR (KBr): 3118, 2226, 1653 cm^{-1}; ^1H NMR (DMSO-d_6, 200 MHz) δ 7.93 (1H, d, J = 1.6 Hz), 7.24 (1H, d, J = 3.8 Hz), 6.07 (1H, m), 4.10 (2H, q, J = 7 Hz), 2.35 (3H, s), 1.05 (3H, t, J = 7 Hz), ^{13}C NMR ($CDCl_3$, 50 MHz): δ 165.3, 160.1, 152.8, 146.3, 146.1, 145.1, 115.8, 115.6, 112.6, 109.6, 96.1, 61.4, 17.9, 13.7; HRMS (EI^+) calculated for $C_{14}H_{12}N_2O_4$: 272.0797, found 272.0797.

*3.1.5. Ethyl-5-cyano-2-methyl-6-oxo-4-(pyridin-4-yl)-1,6-dihydropyridine-3-carboxylate (**6c**)*

Yield: 84%; brown solid; mp 174–176 °C; IR (KBr): 2928, 2228, 1678 cm^{-1}; ^1H NMR (DMSO-d_6, 200 MHz) δ 8.71 (d, J = 5.4 Hz, 2H), 7.08 (d, J = 5.6 Hz, 2H), 3.82 (q, J = 7 Hz, 2H), 2.64 (3H, s), 0.71 (3H, t, J = 7 Hz), ^{13}C NMR ($CDCl_3$, 50 MHz): δ 164.2, 159.5, 157.1, 155.0, 149.8, 144.1, 121.9, 114.9, 110.7, 100.7, 61.1, 18.6, 12.9; HRMS (EI^+) calculated for $C_{15}H_{13}N_3O_3$: 283.0956, found 283.0923.

*3.1.6. Ethyl-5-cyano-2-methyl-4-(2-thienyl)-6-oxo-1,6-dihydropyridine-3-carboxylate (**6d**)*

Yield: 94%; brown solid; mp 212–214 °C; IR (KBr): 2991, 2221, 1655, 1285 cm^{-1}; ^1H NMR (DMSO-d_6, 200 MHz) δ 13.00 (1H, s), 7.86 (d, J = 4.8 Hz, 1H), 7.31 (s, 1H), 7.20 (t, J = 4.2 Hz, 1H), 3.92 (q, J = 7 Hz 2H), 2.36 (s, 3H), 0.89 (t, J = 7 Hz, 3H); ^{13}C NMR ($CDCl_3$, 50 MHz): δ 165.0, 159.7; 152.7, 151.7, 134.9, 129.8, 129.5, 127.7, 115.4, 112.5, 100.6, 61.3, 18.1, 13.3; HRMS (EI^+) calculated for $C_{14}H_{12}N_2O_3S$: 288.0568, found 288.0569.

*3.1.7. Ethyl-4-(3-chlorophenyl)-5-cyano-2-methyl-6-oxo-1,6-dihydropyridine-3-carboxylate (**6e**)*

Yield: 95%; red solid; mp 230–232 °C; IR (KBr): 3331, 2229, 1646 cm^{-1}; ^1H NMR (DMSO-d_6, 200 MHz) δ 7.59 (m, 1H), 7.48 (m, 2H), 7.26 (m, 1H), 3.83 (q, J = 7 Hz, 2H), 2.41 (s, 3H), 0.77 (t, J = 7 Hz, 3H); ^{13}C NMR ($CDCl_3$, 50 MHz): δ 164.5, 159.6, 157.9, 153.9, 138.0, 130.5, 129.3, 127.0, 126.1, 115.2, 111.6, 100.9, 60.9, 18.4, 13.1; HRMS (EI^+) calculated for $C_{16}H_{13}ClN_2O_3$: 316.7390, found 316.7381.

*3.1.8. Ethyl-5-cyano-4-(2,4-dinitrophenyl)-2-methyl-6-oxo-1,6-dihydropyridine-3-carboxylate (**6f**)*

Yield: 85%; red solid; mp 268–269 °C; IR (KBr): 2231, 1677, 1282 cm^{-1}; ^1H NMR (DMSO-d_6, 200 MHz) δ 9.02 (d, J = 1.8, 1H), 8.74 (1H, d, J = 8.4 Hz), 7.83 (d, J = 8.4 Hz, 1H), 3.92 (2H, q, J = 7 Hz); 2.62 (3H, s); 0.90 (t, J = 7 Hz, 3H); ^{13}C NMR ($CDCl_3$, 50 MHz): δ 162.9, 158.9, 157.2, 156.7, 147.8, 146.3, 137.9, 131.3, 128.4, 119.6, 113.9, 108.3, 100.8, 60.9, 19.8, 13.2; HRMS (EI^+) calculated for $C_{16}H_{12}N_4O_7$: 372.0706, found 372.0700.

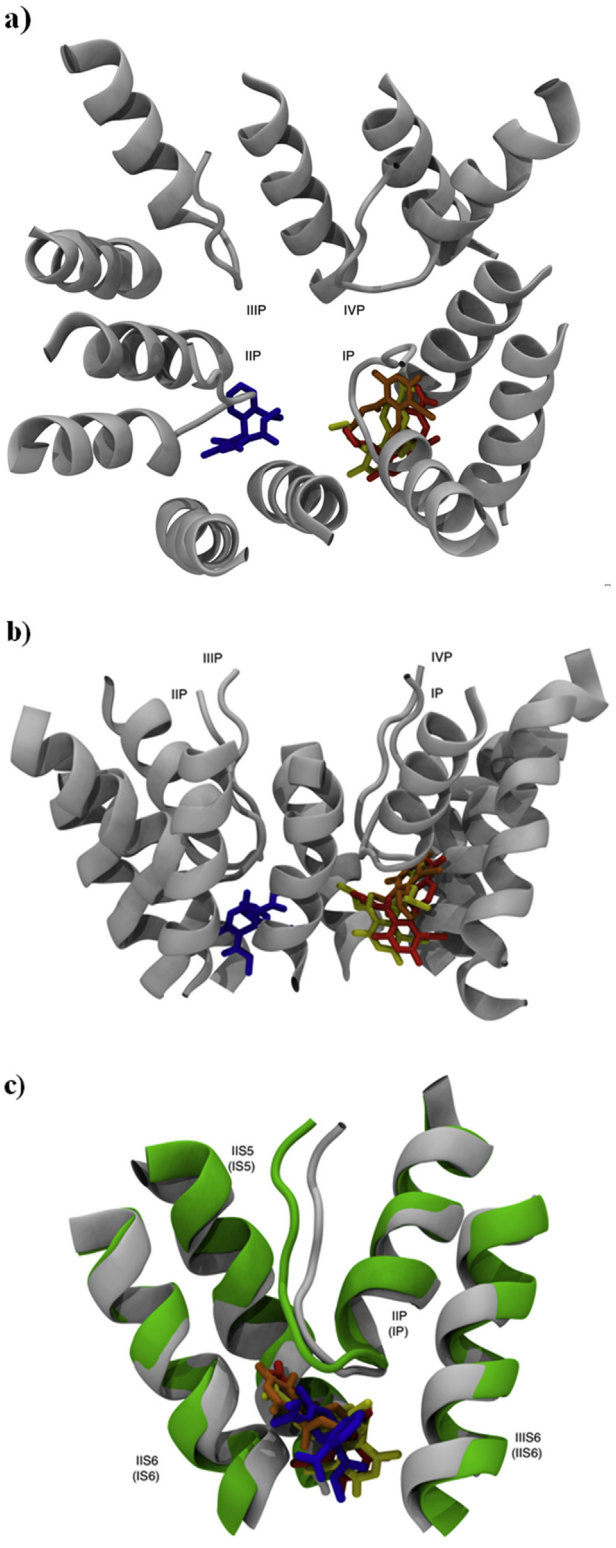

Fig. 4. a) Top view and b) side view of calcium channel model with ligands docked. The ligands are shown on sticks. Nifedipine, **6a** and **d** were docked in the same location. c) Superposition of those helices (white ribbon for cavity conformed for IIS6, IIS5, IIP and IIIS6 helices and green ribbon for cavity of IS6, IS5, IP and IIS6 helices) that conformed the cavities where compounds were docked. Ligands are shown on sticks (nifedipine in blue, **6a** in red, **6d** in orange and **6f** in yellow). (For interpretation of the references to color in this figure legend, the reader is referred to the web version of this article.)

3.2. Vasorelaxant activity

All animals were sacrificed by cervical dislocation and the thoracic aorta was removed, cleaned, and cut in about 3–5 mm length rings. In addition, for some aortic rings the endothelium layer was removed by manual procedures. Then, each piece of tissue was suspended in a tissue chamber containing Krebs

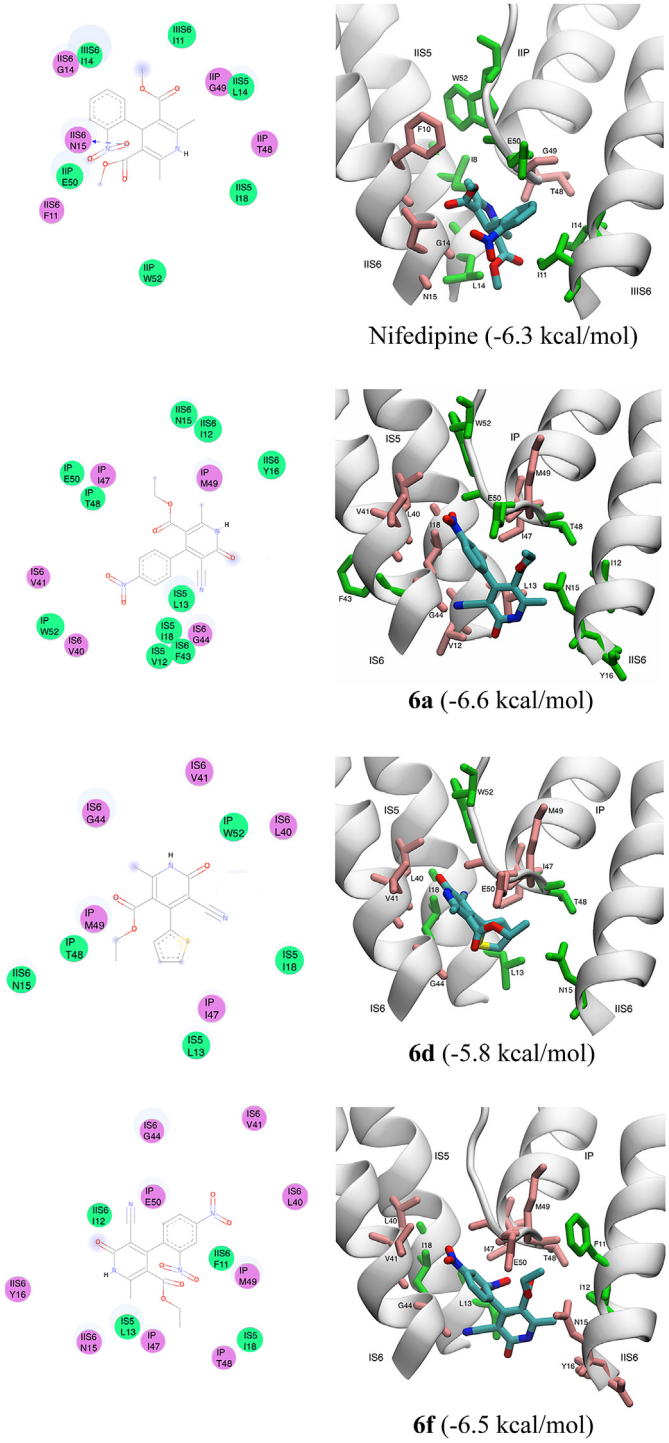

Fig. 5. Protein–ligand interactions diagrams (left) and its corresponding molecular structure representation (right). Circles on green represents non-polar interactions and pink circles polar interactions. (For interpretation of the references to color in this figure legend, the reader is referred to the web version of this article.)

solution at 37 °C, continuously gassed with O_2/CO_2 (9:1). Tissues were placed under a resting tension of 3.0 g and allowed to stabilize for 60 min. The contractions were recorded with an isometrical force transducer Grass FT 03 (Astromed, West Warwick, RI), connected to a MP100 Manager Biopac System polygraph (Biopac Instruments, Santa Barbara, CA). After the stabilization period the tissues were stimulated with NA (0.1 μM) during 10 min and they were washed with fresh Krebs solution. This procedure was repeated three times at 30 min intervals before starting the experiments. The absence or presence of endothelium layer was confirmed by the lack of the relaxant response induced by carbachol (1 μM) in the last contraction to assess viability. Finally, all tissues were contracted with NA and test samples (pure compounds or positive control) were added to the bath in quarter-log cumulative concentrations (evaluation period). The relaxant effect of the samples was determined by its ability to induce a maximal vascular contraction before and after their addition.

3.3. Docking

Lipkind's molecular model of calcium channel L-type was kindly obtained from Prof. Mancilla-Percino et al., 2010 [30]. The sequence present on the original structure was modified to be on agreement with NCBI sequence NP_005174.2 for subunit alpha-1F isoform 1. Missing hydrogens were built and the final channel structure energy minimized with 250 steps of steepest descent method using Amber ff99SB parameters [31] as implemented on Chimera USCF software [32]. Nifedipine, **6a**, **d** and **f** compounds were built using Avogadro software version 1.1.0 [33]. Geometry optimization of each ligand was done using RM1 method for MOPAC [34] as implemented on Avogadro. Pymol [35] and Autodock/Vina plugin for PyMOL were used to prepare all the necessary files for docking [36]. Only polar atoms were used for protein. Protein grid was centered at (0.5, 0.42, 5.2) with dimensions of the grid of 28 × 32 × 22 with a spacing of 1 Å between grid points with exhaustiveness of 48. Docking was performed by Autodock Vina version 1.1.2 [37]. Protein–ligand diagram interactions were done using Discovery Studio Visualizer [38] and all molecular structures with VMD [39].

Acknowledgments

This study was financed by a grant from "Apoyo a la Mejora del Perfil Individual del profesorado de tiempo completo (Fondo para la Consolidación de las Universidades Públicas Estatales y con Apoyo Solidario Ejercicio 2009)" and Faculty of Pharmacy Budgets (FECES 2011 and 2012). F.H. thanks CONACyT for a graduate scholarship (no. 482137) M.A.V. acknowledges CONACyT (grant 168474) and UGto-DAIP (grant 281/13).

Appendix A. Supplementary data

Supplementary data related to this article can be found at http://dx.doi.org/10.1016/j.ejmech.2013.10.018.

References

[1] V. Sharma, J.H. McNeill, The etiology of hypertension in the metabolic syndrome part one: an introduction to the history, the concept and the models, Curr. Vasc. Pharmacol. 4 (2006) 293–304.
[2] J.C. Russell, S.D. Proctor, Small animal models of cardiovascular disease: tools for the study of the roles of metabolic syndrome, dyslipidemia, and atherosclerosis, Cardiovasc. Pathol. 15 (2006) 318–330.
[3] D.H. Endemann, E.L. Schiffrin, Endothelial dysfunction, J. Am. Soc. Nephrol. 15 (2004) 1983–1992.
[4] B.A. Staffileno, Treating hypertension with cardioprotective therapies: the role of ACE inhibitors, ARBs, and beta-blockers, J. Cardiovasc. Nurs. 20 (2005) 354–364.
[5] M. Ravinder, B. Mahendar, S. Mattapally, K.V. Hamsini, T.N. Reddy, C. Rohit, K. Srinivas, S.K. Banerjee, V.J. Rao, Synthesis and evaluation of novel 2-pyridone derivatives as inhibitors of phosphodiesterase 3 (PDE3): a target for heart failure and platelet aggregation, Bioorg. Med. Chem. Lett. 22 (2012) 6010–6015.
[6] P.E. Thompson, V. Manganiello, E. Dergerma, Re-discovering PDE3 inhibitors – new opportunities for a long neglected target, Curr. Top. Med. Chem. 4 (2007) 421–436.
[7] A.H. Abadi, D.A. Abouel-Ella, J. Lehmann, H.N. Tinsley, B.D. Gary, G.A. Piazza, M.A.O. Abdel-Fattah, Discovery of colon tumor cell growth inhibitory agents through a combinatorial approach, Eur. J. Med. Chem. 45 (2010) 90–97.
[8] A. Lundy, N. Lutfi, C. Beckey, Review of nifedipine GITS in the treatment of high risk patients with coronary artery disease and hypertension, Vasc. Health Risk Manag. 5 (2009) 429–440.
[9] Y. Chen, H. Zhang, F. Nan, Construction of a 3-amino-2-pyridone library by ring-closing metathesis of alpha-amino acrylamide, J. Comb. Chem. 6 (2004) 684–687.
[10] S. Wang, T. Tan, J. Li, H. Hu, Highly efficient one-pot synthesis of 1,2-Dihydro-2-oxo-3-pyridine-carboxylate derivatives by $FeCl_3$-promoted [3+3] annulation, Synlett (2005) 2658–2660.
[11] J.L. Soto, C. Seoane, P. Zamorano, M.J. Rubio, A. Monforte, M. Quinteiro, Synthesis of hetero cyclic compounds. Part 46. The reactions of malonamide and 2-cyanoacetamide with substituted propenones, J. Chem. Soc. Perkin Trans. (1985) 1681–1685.
[12] X. Dexuan, W. Kewei, L. Yongjiu, Z. Guangyuan, D. Dewen, A facile and efficient synthesis of polyfunctionalized pyridin-2(1*H*)-ones from α-oxo amides under Vilsmeier conditions, Org. Lett. 10 (2008) 345.
[13] Y.S. Chun, K.Y. Ryu, Y.O. Ko, J.Y. Hong, J. Hong, H. Shin, S.G. Lee, One-pot synthesis of 2-pyridones via chemo- and regioselective tandem Blaise reaction of nitriles with propiolates, J. Org. Chem. 74 (2009) 7556–7558.
[14] R. Miranda, O. Noguez, B. Velasco, G. Arroyo, G. Penieres, J. Martínez, F. Delgado, Irradiación infrarroja: una alternativa para la activación de reacciones y su contribución a la Química Verde, Educ. Quím. 20 (2009) 421–425.
[15] F. Delgado, J. Tamariz, G. Zepeda, M. Landa, R. Miranda, J. García, Knoevenagel condensation catalyzed by a Mexican Bentonite using infrared irradiation, Synth. Commun. 25 (1995) 753–759.
[16] E. Obrador, M. Castro, J. Tamariz, G. Zepeda, R. Miranda, F. Delgado, Knoevenagel condensation in heterogenous phase catalyzed by IR radiation, Synth. Commun. 28 (1998) 4649–4663.
[17] G. Alcerraca, R. Sanabria, R. Miranda, G. Arroyo, F. Delgado, Preparation of benzylidene barbituric acids promoted by infrared irradiation in absence of solvent, Synth. Commun. 30 (2000) 1295–1301.
[18] R. Gómez, R. Osnaya, I. Zamora, B. Velasco-Bejarano, G. Arroyo, E. Ramírez-San Juan, J. Trujillo, F. Delgado, R. Miranda, The Hantzsch ester production in a water-based biphasic medium, using infrared irradiation as the activating source, J. Mex. Chem. Soc. 51 (2007) 181–184.
[19] M.A. Vázquez, M. Landa, L. Reyes, R. Miranda, J. Tamariz, F. Delgado, Infrared irradiation: effective promoter of *N*-benzylideneanilines under solventless conditions, Synth. Commun. 34 (2004) 2705–2718.
[20] A. Sánchez, F. Hernández, P. Cruz, Y. Alcaraz, J. Tamariz, F. Delgado, M.A. Vázquez, Infrared irradiation-assisted multicomponent synthesis of 2-amino-3-cyano-4*H*-pyran derivatives, J. Mex. Chem. Soc. 56 (2012) 121–127.
[21] M.I. Flores-Conde, L. Reyes, R. Herrera, H. Rios, M.A. Vazquez, R. Miranda, J. Tamariz, F. Delgado, Highly regio- and stereoselective Diels-Alder cycloadditions via two-step and multicomponent reactions promoted by infrared irradiation under solvent-free conditions, Int. J. Mol. Sci. 13 (2012) 2590–2617.
[22] P. Bhattacharyya, K. Pradhan, S. Paul, A.R. Das, Nano crystalline ZnO catalyzed one pot multicomponent reaction for an easy access of fully decorated 4*H*-pyran scaffolds and its rearrangement to 2-pyridone nucleus in aqueous media, Tetrahedron Lett. 23 (2012) 4687–4691.
[23] G.C. Pool, J.H. Teuben, IR radiation as a heat source in vacuum sublimation, in: A.L. Wayda, M.Y. Darensbourg (Eds.), Practical Organometallic Chemistry, Symposium Series, vol. 357, 1987, pp. 30–33. Washington, D.C.
[24] F. Orallo, E. Alvarez, H. Basaran, C. Lugnier, Comparative study of the vasorelaxant activity, superoxide-scavenging ability and cyclic nucleotide phosphodiesterase-inhibitory effects of hesperetin and hesperidin, Naunyn–Schmiedebergs Arch. Pharmacol. 370 (2004) 452–463.
[25] J. Vergara-Galicia, R. Ortiz-Andrade, J. Rivera-Leyva, P. Castillo-España, R. Villalobos-Molina, M. Ibarra-Barajas, I. Gallardo-Ortiz, S. Estrada-Soto, Vasorelaxant and antihypertensive effects of methanolic extract from roots of *Laelia anceps* are mediated by calcium-channel antagonism, Fitoterapia 81 (2010) 350–357.
[26] A. Pandey, P. Jigneshkumar, S. Tripathi, C.G. Mohan, Harnessing human n-type Ca^{2+} channel receptor by identifying the atomic hotspot regions for its structure-based blocker design, Mol. Inf. 31 (2012) 643–657.
[27] S. Cosconati, L. Marinelli, A. Lavecchia, E. Novellino, Characterizing the 1,4-dihydropyridines binding interactions in the L-type Ca^{2+} channel: model construction and docking calculations, J. Med. Chem. 50 (2007) 1504–1513.

[28] G.M. Lipkind, H.A. Fozzard, Molecular modeling of interactions of dihydropyridines and phenylalkylamines with the inner pore of the L-type Ca^{2+} channel, Mol. Pharmacol. 63 (2003) 499–511.
[29] S. Goldmann, J. Stoltefuss, 1,4-Dihydropyridines: effects of chirality and conformation on the calcium antagonist and calcium agonist activities, Angew. Chem. Int. Ed. 30 (1991) 1559–1578.
[30] T. Mancilla-Percino, J. Correa-Basurto, J. Trujillo-Ferrara, F.R. Ramos-Morales, M.E. Acosta Hernández, J.S. Cruz-Sánchez, M. Saavedra-Vélez, Molecular modeling study of isoindolines as L-type Ca(2+) channel blockers by docking calculations, J. Mol. Model. 16 (2010) 1377–1382.
[31] W.D. Cornell, P. Cieplak, C.I. Bayly, I.R. Gould, K.M. Merz, D.M. Ferguson, D.C. Spellmeyer, T. Fox, J.W. Caldwell, P.A. Kollman, A second generation force field for the simulation of proteins, nucleic acids, and organic molecules, J. Am. Chem. Soc. 117 (1995) 5179–5197.
[32] E.F. Pettersen, T.D. Goddard, C.C. Huang, G.S. Couch, D.M. Greenblatt, E.C. Meng, T.E. Ferrin, Chimera – a visualization system for exploratory research and analysis, J. Comput. Chem. 25 (2004) 1605–1612.
[33] M.D. Hanwell, D.E. Curtis, D.C. Lonie, T. Vandermeersch, E. Zurek, G.R. Hutchison, Avogadro: an advanced semantic chemical editor, visualization, and analysis platform, J. Chemin. 4 (2012) 17.
[34] J.P.S. James, MOPAC: a general molecular orbital package, Quant. Chem. Prog. Exch. 10 (1990) 86.
[35] L. Schrödinger, The PyMOL Molecular Graphics System, Version 1.3r1, LCC, 2010.
[36] D. Seeliger, B.L. De Groot, Ligand docking and binding site analysis with PyMOL and Autodock/Vina, J. Comput. Aided Mol. Des. 24 (2010) 417–422.
[37] O. Trott, A.J. Olson, AutoDock Vina: improving the speed and accuracy of docking with a new scoring function, efficient optimization, and multithreading, J. Comput. Chem. 31 (2010) 455–461.
[38] Discovery Studio Modeling Environment, Accelrys Software Inc., San Diego, 2012.
[39] W. Humphrey, A. Dalke, K. Schulten, VMD – visual molecular dynamics, J. Mol. Graph. 14 (1996) 33–38.